


An Investigation of the Mechanisms of Radiation-Induced Muscle Injury in a Tree Shrew (*Tupaia belangeri*) Model

Dose-Response:
An International Journal
January-March 2022:1–10
© The Author(s) 2022
Article reuse guidelines:
sagepub.com/journals-permissions
DOI: 10.1177/15593258221082878
journals.sagepub.com/home/dos


Pengcheng Zhao^{1,2,*} , Wei Xia^{1,2,*}, Jianglian Wei^{1,2}, Yiwei Feng^{1,2}, Mao Xie^{1,2}, Zhijie Niu^{1,2}, Heng Liu³, Shenghui Ke^{1,2}, Huayu Liu^{1,2}, Anzhou Tang^{1,2}, and Guangyao He^{1,2}

Abstract

Background: Animal models suitable for investigating mechanisms behind radiation-induced muscle injury are lacking. We developed a tree shrew model of such injury and investigated pathological changes and mechanisms.

Methods: Animals were divided into control (n = 5), radiation-induced acute injury (n = 5), and radiation-induced chronic injury (n = 5) groups. Tensor veli palatini (TVP) muscles of acute injury and chronic injury groups were dissected under a microscope at 1 and 24 weeks after radiation therapy, respectively. TVP muscles were stained with HE and Masson to visualize pathological changes. ELISA was performed to measure oxidative injury. RT-qPCR and immunohistochemical staining was performed to measure expression levels of miR-206 and histone deacetylase 4 (HDAC4).

Results: Compared to the control group, acute injury group showed a significant decrease in miR-206 expression ($.061 \pm .38$, $P < .05$) and a significant increase in HDAC4 expression (37.05 ± 20.68 , $P < .05$). Chronic injury group showed a significant decrease in miR-206 expression ($.23 \pm .19$, $P < .05$) and a significant increase in HDAC4 expression (9.66 ± 6.12 , $P < .05$).

Discussion: A tree shrew model of radiation-induced muscle injury was established by exposing TVP muscle region to radiation of 20-Gy. Experimental results indicated that injury caused by radiation persisted despite gradual healing of the TVP muscle and miR-206 regulatory pathway plays a key role in regulating radiation-induced muscle injury.

Keywords

dose response, nasopharyngeal carcinoma, radiation-induced muscle injury, gene expression

Introduction

Nasopharyngeal carcinoma (NPC) is a malignant neoplasm originating from the mucosal epithelium of the nasopharynx. Its geographical distribution is characterized by distinct regionality, with Southeast Asian countries having a particularly high incidence of 2.54/100,000 population per year (2017 data).^{1,2} Radiation-based combination therapy is currently the most commonly used treatment method for NPC,³ with patients treated with radiation therapy showing 5-year and 10-year overall survival rates of approximately 76.1% and 66.5%, respectively.⁴ However, radiation not only kills malignant proliferative tumor tissues but also causes injury to the surrounding normal tissues, resulting in radiation-induced bone

¹Department of Otolaryngology–Head and Neck Surgery, The First Affiliated Hospital of Guangxi Medical University, Nanning, China

²Key Laboratory of Early Prevention and Treatment for Regional High Frequency Tumor, Ministry of Education, Nanning, China

³School of Information and Management, Guangxi Medical University, Nanning, China

*Pengcheng Zhao and Wei Xia contributed equally to this work and should be considered co-first authors.

Corresponding Authors:

Anzhou Tang, Department of Otolaryngology–Head and Neck Surgery, The First Affiliated Hospital of Guangxi Medical University, shuangyong Road, Nanning 530021, China.

Email: AnzhouTang@126.com

Guangyao He, Department of Otolaryngology–Head and Neck Surgery, The First Affiliated Hospital of Guangxi Medical University, shuangyong Road, Nanning 530021, China.

Email: 6118361@qq.com



Creative Commons Non Commercial CC BY-NC: This article is distributed under the terms of the Creative Commons Attribution-NonCommercial 4.0 License (<https://creativecommons.org/licenses/by-nc/4.0/>) which permits non-commercial use, reproduction and distribution of the work without further permission provided the original work is attributed as specified on the SAGE

and Open Access pages (<https://us.sagepub.com/en-us/nam/open-access-at-sage>).

injury, vascular, and muscle injuries.⁵⁻⁷ Among these, radiation-induced muscle injury is closely associated with the onset of symptoms and long-term complications such as radiotherapy-induced secretory otitis media, dropped head syndrome, neck pain, and dysphagia.⁸⁻¹¹

After muscle injury, satellite cells in the skeletal muscle are activated and undergo proliferation and fusion to form myotubes that, in turn, differentiate to mature muscle fibers to replace the lost muscle fibers. Disruption of the repair process causes capillary injury, sarcolemmal damage, and muscle fibrosis, which results in long-term muscle injury.¹² Micro-RNA (miR)-206, a skeletal muscle-specific miRNA, participates in the repair process following muscle injury in muscle-related diseases such as rhabdomyosarcoma and amyotrophic lateral sclerosis¹³⁻¹⁵ by regulating histone deacetylase 4 (HDAC4), which is a downstream target.¹⁶ Therefore, downregulation of miR-206 may lead to incomplete muscle repair after injury.

The tree shrew (*Tupaia belangeri*), a small mammal species, is more closely genetically related to primates compared to conventional rodents. Therefore, it has been used in the construction of animal models of hepatocellular carcinoma and viral hepatitis.¹⁷⁻¹⁹ Gao et al. found that radiation-induced impairment of the tensor veli palatine (TVP) muscle function is associated with post-radiation secretory otitis media.²⁰ In our previous study, we established a tree shrew model of secretory otitis media by subjecting the TVP muscles to two different types of treatment. Our results indicated that the TVP muscle in the tree shrew functions similarly to humans to open the Eustachian tube. Furthermore, we found that secretory otitis media was caused by Eustachian tube dysfunction, with the histopathological changes occurring in the tree shrew like those in humans.²¹ In the present study, we irradiated the TVP muscle of tree shrews to develop an animal model to investigate the pathogenesis of radiation-induced muscle injury. The results of this study may serve as a scientific basis for future research and treatment of complications caused by radiation-induced muscle injury.

Materials and Methods

Experimental Animals

Fifteen normal clean-grade tree shrews of both sexes aged 12 months with body weights of 120–150 g each were purchased from the Kunming Institute of Zoology and reared in a clean-grade animal room in the Laboratory Animal Center of Guangxi Medical University. After 2 weeks of acclimatization, the tree shrews were randomly divided into the radiation-induced acute injury (R-1w, n = 5), radiation-induced chronic injury (R-24w, n = 5), and control (C, n = 5) groups and subjected to experimentation. The study was approved by the Experimental Animal Ethics Committee of Guangxi Medical University (Approval No:20,210,2003) and conducted in strict compliance with the Guide for the Care and Use of Laboratory Animals.

Radiation Therapy

In the previous study, we performed 10 Gy, 20 Gy, 30 Gy, and 40 Gy radiation on the tensor veli palatine muscle of the tree shrew, respectively. By counting tree shrew mortality and observing the tensor veli palatine muscle's pathological changes, we chose a dose of 20 Gy in this study. Before receiving radiation therapy, the tree shrews in all three groups were anesthetized via intraperitoneal injection of 1% pentobarbital sodium (65 mg/kg).²² Each tree shrew in the radiation-induced chronic and acute injury groups was placed in the left lateral recumbent position with the right ear facing upwards. The right TVP muscle region was irradiated once with a 9 MeV electron beam produced by a linear particle accelerator (Varian Clinac iX, SN4948, software version 9.01; Varian Medical Systems, California, USA) using the following parameters: total radiation dose: 20 Gy, radiation field: 2 cm × 5 cm, source-to-skin distance: 100 cm, depth: 1.9 cm. After irradiation, the tree shrews were returned to their rearing cages and placed in the lateral recumbent position to prevent asphyxiation until natural recovery from anesthesia. The tree shrews in the control group were reared in the same manner as the other two groups except that irradiation was not performed.

Observations and Specimen Collection

After irradiation, the body weight, hair appearance, food intake, and water intake of the tree shrews in all three groups were observed. The tree shrews in the radiation-induced acute and chronic injury groups were euthanized via an overdose of sodium pentobarbital administered by injection at 1 and 24 weeks after irradiation, respectively. Following dissection of the TVP muscle, one portion of the muscular tissue was fixed in 10% neutral buffered formalin (PH0996; Phygene Biotech Company, Fuzhou, China); the remaining muscular tissue was placed in a 2 mL cryogenic tube and stored at –80°C.

Hematoxylin and Eosin Staining

The TVP muscle samples that had been fixed for 24 h were dewatered routinely, embedded in paraffin, sectioned into 4 μm slices, dewaxed, and stained using an H&E stain kit (G1120; Solarbio Science and Technology Company, Beijing, China). Morphological changes in the TVP muscle were observed at ×400 magnification under an optical microscope (B×53-F; Olympus, Tokyo, Japan).

Capillary Counting

Five fields of view (FOVs) were randomly selected from each of three randomly selected H&E stained sections of each of three randomly selected animals from each group. Individual capillaries formed from capillary endothelial cells were observed at 1000× magnification under an optical microscope, and the number of capillaries was counted at 400×

Table 1. Primer sequence of the marker genes.

Gene name	Forward primers (5'to3')	Reverse primers (5'to3')
miR-206	GGGTGGAATGTAAGGAAGT	TGCGTGTCTGGAGTC
HDAC4	GTGAAGCAGGAGCCCATT	GGAGGGCTTGCTGTCTGA
u6	TCGCTTC-GGCAGCACATA	AATTTGCGTGTCTCCTTGC
β -actin	CGGGAAATTGTGCGTGACAT	AGATTCCATGCCAGGAAAGA

magnification. The capillary count was obtained by calculating the average value.

Masson's Trichrome Staining

TVP muscle sections were dewaxed and stained using a Masson's trichrome staining kit (G1340; Solarbio Science and Technology Company, Beijing, China). This staining method allows for the differentiation of muscle and collagen fibers, as low-molecular-weight anionic dyes (e.g., ponceau-acid fuchsin) can penetrate tissues with low permeability while high molecular weight anionic dyes (eg, aniline blue) can only penetrate tissues with high permeability. Therefore, muscle fibers appear red and collagen fibers appear blue after staining. The degree of fibrosis in the TVP muscle was observed at 400 \times under a microscope and compared among the three groups using Image-Pro Plus 6.0 (Media Cybernetics, Bethesda, USA).

Enzyme Linked Immunosorbent Assay

A total of 20 mg of muscle tissue was thoroughly homogenized in 500 μ l phosphate-buffered saline (PBS). The supernatant obtained from homogenization was removed and separately subjected to ELISA using malondialdehyde (MDA) (YBE-9903; Yu Bo Biotech Company, Shanghai, China) and superoxide dismutase (SOD) (YBE-0771; Yu Bo Biotech Company, Shanghai, China) ELISA kits to measure the MDA and SOD levels in muscle tissue.

Reverse Transcription-Quantitative Real-Time Polymerase Chain Reaction

A total of 30 mg of muscle tissue was lysed using QIAzol lysis reagent (79,306; QIAGEN, Germany) and total RNA was extracted using the miRNeasy Mini Kit (21,7004; QIAGEN, Germany). Reverse transcription was performed with the miRcute Plus miRNA First-Strand cDNA kit (KR211; TianGen Biotech Company, Beijing, China) using 500 ng of RNA as the starting material. miR-206 expression was measured by fluorescence-based qPCR according to the instructions provided with the miRcute Plus miRNA qPCR kit (SYBR Green) (FP411; TIANGEN Biotech Co., Ltd., Beijing, China), with U6 used as the housekeeping gene. Relative expression levels were calculated using the $2^{-\Delta\Delta CT}$ method ($\Delta CT = CT_{miR206} - CT_{u6}$).

The total RNA was reverse transcribed using the Fastking gDNA Dispelling RT SuperMix (KR118; TIANGEN Biotech Co., Ltd., Beijing, China). HDAC4 expression was measured by fluorescence-based qPCR according to the instructions provided with the Talent qPCR PreMix (SYBR Green) (FP209; TianGen Biotech Company, Beijing, China), with β -actin used as the housekeeping gene. The relative expression levels were calculated using the $2^{-\Delta\Delta CT}$ method ($\Delta CT = CT_{HDAC4} - CT_{\beta\text{-actin}}$).

The primers were synthesized by Sangon Biotech (Shanghai) Co., Ltd. Table 1 shows the primer sequences of the marker genes.

Immunohistochemical Staining

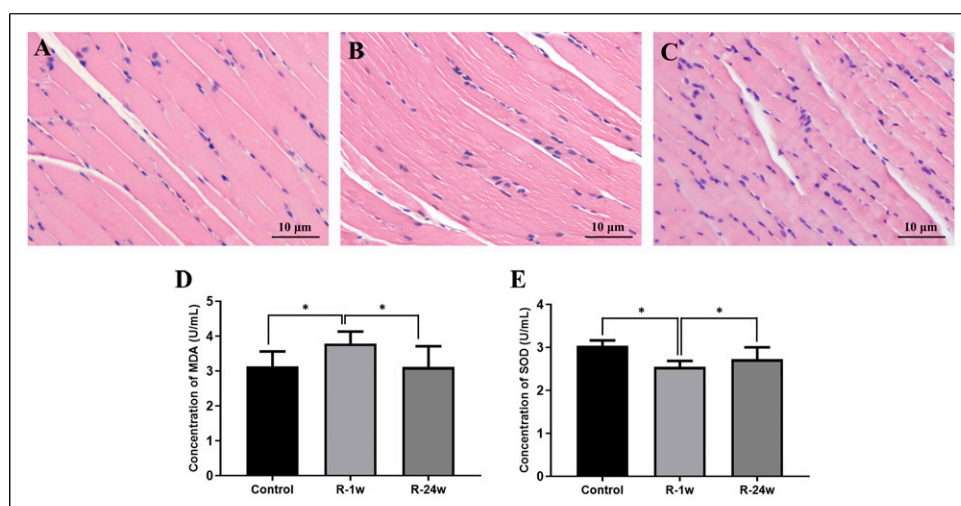
Muscle tissue sections of the three groups were subjected to immunohistochemical staining. Before experimentation, high-pressure antigen retrieval was performed using sodium citrate buffer (pH = 6.0). The sections were then incubated at 37°C for 1 h using a mouse/rabbit streptavidin-biotin detection system test kit (SP-9000; Beijing Zhongshan Golden Bridge Biotechnology Co. Ltd, Beijing, China), using anti-mouse HDAC4 polyclonal antibody at a dilution of 1:300 as the primary antibody (NPB2-22151; Novus, Minneapolis, USA). This was followed by incubation with diaminobenzidine (DAB) staining solution (P0203; Beyotime Biotechnology, Jiangsu, China) at 25°C for 5 min, staining with hematoxylin staining solution (PH0425; Phygene Biotech Company, Fuzhou, China), and routine dewatering and mounting. HDAC4 expression was observed under a microscope at 400 \times magnification. Five fields of view (FOVs) were randomly selected from each of three randomly selected sections of each of three randomly selected animals from each group for the comparison of areas with positive expression.

Statistical Analysis

Data were processed and statistically analyzed using IBM SPSS Statistics for Windows, version 25.0. Quantitative data were expressed as means \pm standard deviation. Comparisons of two groups were performed using t-tests, and comparisons of multiple groups were performed by analysis of variance (ANOVA). Differences were considered statistically significant for $P < .05$.

Table 2. General characteristics of the three study groups.

Group	Number	Sex	Weight(g)	Experiment method, Gy	End time
Control group	1	Male	131	0	0 w
	2	Female	133.9		
	3	Female	135.5		
	4	Female	129.6		
	5	Male	132.5		
Radiation-induced acute injury group	1	Female	124.9	20	1 w
	2	Male	125.2		
	3	Male	124		
	4	Male	129.8		
	5	Female	126.7		
Radiation-induced chronic injury group	1	Male	129.8	20	24 w
	2	Male	126.7		
	3	Male	128		
	4	Female	128.1		
	5	Female	130.9		

**Figure 1.** Radiation-induced TVP muscle injury (200 \times). A: H & E stain of control group; B: H & E stain of radiation-induced acute injury group; C: H & E stain of radiation-induced chronic injury group; D: MDA expression; E: SOD expression. Control: control group; R-1w: radiation-induced acute injury group; R-24 w: radiation-induced chronic injury group. *: P < .05.

Results

General Status

The radiation-induced chronic injury group had a slightly lower body weight compared to that in the control group (128.70 ± 1.70 g vs 132.50 ± 2.30 g, $P > .05$). The body weight of the radiation-induced chronic injury group was slightly higher than that in the radiation-induced acute injury group ($P > .05$) (Table 2). After irradiation, the hair behind the ear on the irradiated side gradually turned white in the radiation-induced acute injury group, while the hair behind the ear, as well as the neck, gradually turned white in the radiation-induced chronic injury group. No abnormalities in food and water intake were observed in all three groups.

Radiation-Induced Muscle Injury

The H & E staining revealed the following: (1) Control group: intact sarcolemma in the muscles, regular muscle fiber morphology with uniform fiber thicknesses and orderly arrangement of nuclei near the edge of the sarcolemma; (2) Radiation-induced acute injury group: disordered muscle fiber morphology in the muscle tissue, pyknosis in some nuclei, and capillary swelling; (3) Radiation-induced chronic injury group: slight loss of sarcolemma in the muscle tissue, increased gaps between muscle fibers, slightly loose connective tissue structures around the muscle, and increased nuclei aggregation. Both the radiation-induced acute injury and chronic injury groups showed injury compared to the control group (Figures 1A–C).

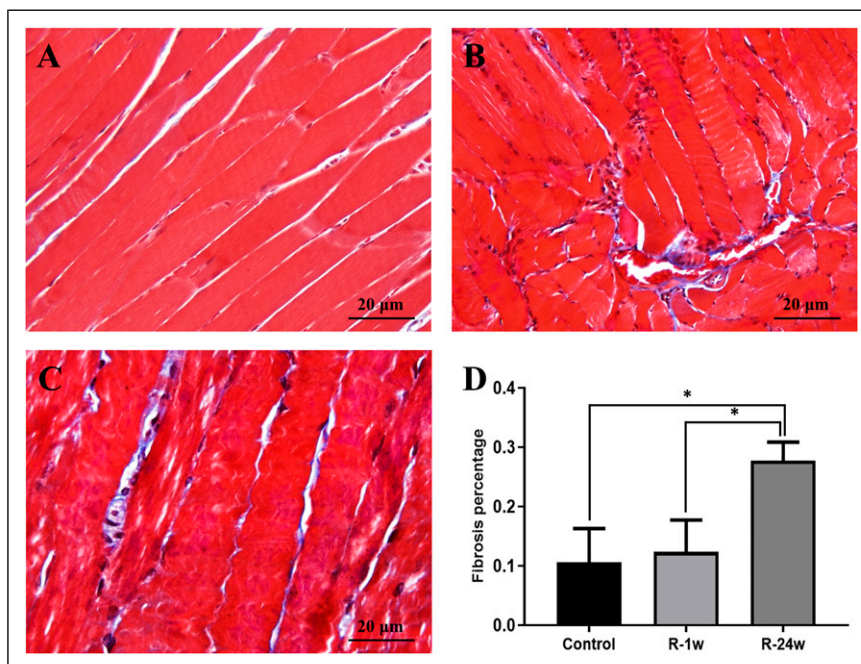


Figure 2. Masson's trichrome stains of radiation-induced TVP muscle injury, with collagen fibers stained blue and muscle fibers stained red (400 \times). A: control group; B: radiation-induced acute injury group; C: radiation-induced chronic injury group; D: Percentage of area occupied by collagen fibers. Control: control group; R-1 w: radiation-induced acute injury group; R-24 w: radiation-induced chronic injury group. *: $P < .05$.

The ELISA results showed significantly higher MDA expression in the radiation-induced acute injury group compared to the control group ($3.79 \pm .35$ U/mL vs $3.12 \pm .59$ U/mL, $P < .05$). The radiation-induced chronic injury group showed a moderate increase in MDA expression compared to the control group ($3.13 \pm .43$ U/mL vs $3.12 \pm .59$ U/mL, $P > .05$) but a significant decrease compared to the radiation-induced acute injury group ($P < .05$). Compared to the control group, the radiation-induced acute injury group showed a significant decrease in SOD expression ($3.04 \pm .12$ U/mL vs $2.55 \pm .14$ U/mL, $P < .05$). The radiation-induced chronic injury group showed a moderate decrease in SOD expression compared to the control group ($2.73 \pm .28$ U/ml, $P > .05$) but a significant increase compared to the radiation-induced acute injury group ($P < .05$) (Figures 1D and E). These results suggested more severe oxidative injury in the radiation-induced acute injury group compared to that in the radiation-induced chronic injury group, while the oxidative injury of the latter group was gradually repaired. This demonstrates the presence of chronic injury and repair in addition to acute injury in muscles subjected to irradiation.

Radiation-Induced Muscle Fibrosis

Compared to the control group, the radiation-induced acute injury group did not show significant fibrosis in the muscle tissue ($.11 \pm .058$ vs $.12 \pm .054$, $P > .05$) while the radiation-induced chronic injury group showed a significant increase in the degree of fibrosis ($.11 \pm .058$ vs $.28 \pm .031$, $P < .05$).

Compared to the radiation-induced acute injury group, the radiation-induced chronic injury group showed a significantly higher degree of fibrosis ($P < .05$) (Figure 2). This indicated that muscle fibrosis was more prominent in the radiation-induced chronic injury group than the acute injury group.

Radiation-Induced Vascular Injury

Compared to the control group, both the radiation-induced acute injury and chronic injury groups showed significantly reduced capillary densities (both $P < .05$). However, the radiation-induced chronic injury group had a significantly higher capillary density than the radiation-induced acute injury group ($P < .05$) (Figure 3A–C). Masson's trichrome staining also revealed collagen fiber hyperplasia around the capillaries of the radiation-induced acute and chronic injury groups compared to the control group (Figures 3E–G). This indicated that the decrease in capillary count mainly occurred during the acute phase of radiation-induced injury. Over time, the number of capillaries gradually increased; however, fibrosis also occurred around the capillaries.

miR-206 and HDAC4 Gene Expression in Muscle

The RT-qPCR showed significantly lower miR-206 expression in both the radiation-induced acute injury ($.061 \pm .38$, $P < .05$) and radiation-induced chronic injury ($.23 \pm .19$, $P < .05$) groups compared to the control group. The radiation-induced

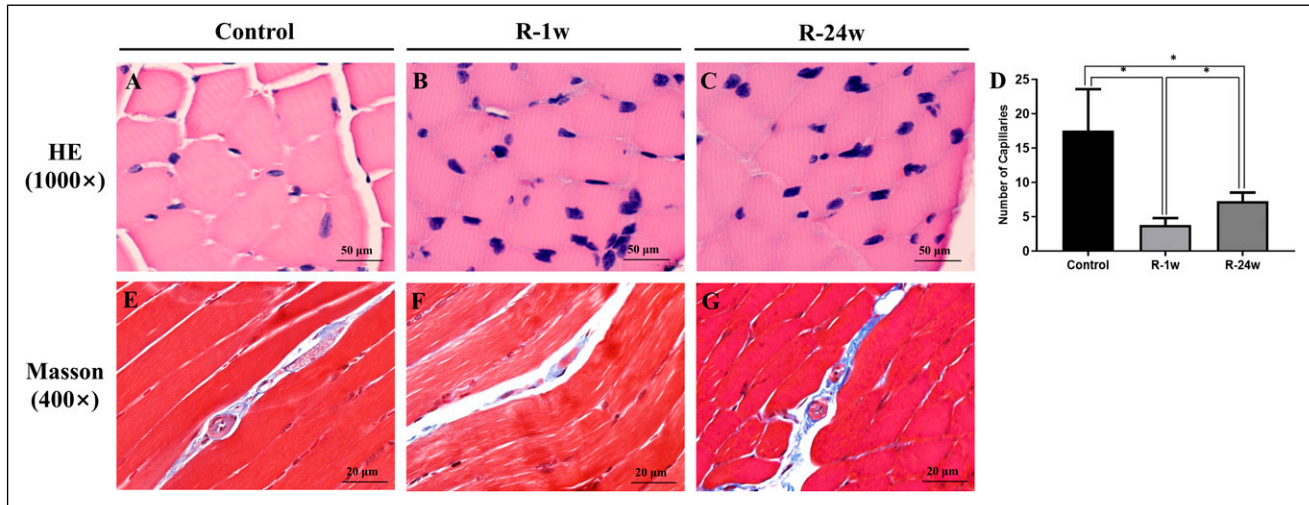


Figure 3. Capillary density (1000 \times) and fibrosis (400 \times) in radiation-induced TVP muscle injury. A, E: control group; B, F: radiation-induced acute injury group; C, G: radiation-induced chronic injury group; D: Analysis of capillary density. Control: control group; R-1 w: radiation-induced acute injury group; R-24 w: radiation-induced chronic injury group. *: $P < .05$.

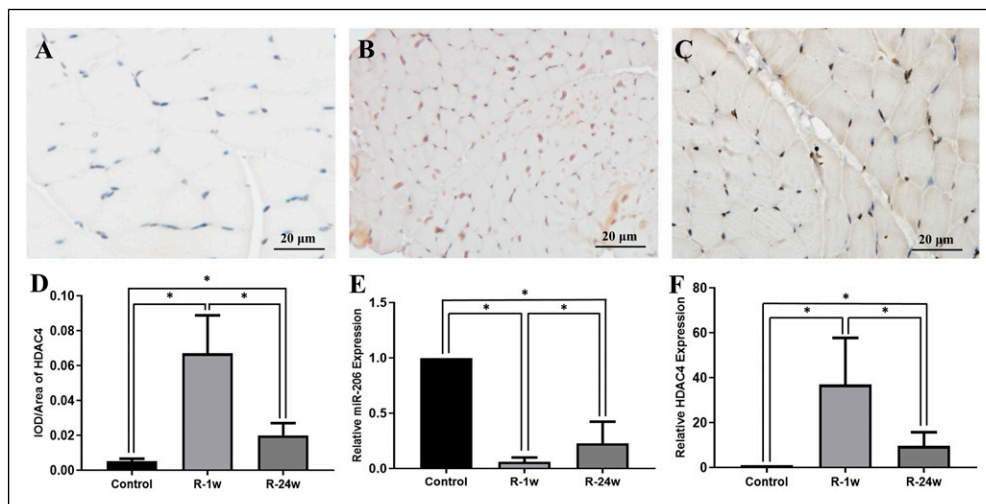


Figure 4. miR-206 and HDAC4 gene and protein expression in radiation-induced TVP muscle injury (400 \times). A: control group; B: radiation-induced acute injury group; C: radiation-induced chronic injury group; D: Analysis of positive HDAC4 expression; E: miR-206 expression; F: HDAC4 expression. Control: control group; R-1 w: radiation-induced acute injury group; R-24 w: radiation-induced chronic injury group. *: $P < .05$.

chronic injury group also showed a significant increase in miR-206 expression compared to the radiation-induced acute injury group ($P < .05$).

HDAC4 is a key target gene in the regulation of muscle injury repair by miRNAs. The RT-qPCR results indicated that compared to the control group, the radiation-induced acute injury group showed a significant increase in HDAC4 expression (37.05 ± 20.68 , $P < .05$) while the radiation-induced chronic injury group showed a significant decrease in HDAC4 expression (9.66 ± 6.12 , $P < .05$). Compared to the radiation-induced acute injury group, the radiation-induced chronic injury group showed significantly lower HDAC4 expression

($P < .05$) (Figure 4E and F). These results demonstrated the downregulation of miR-206 during radiation-induced injury, leading to an increase in downstream HDAC4 expression. During muscle injury repair, miR-206 expression was upregulated, resulting in decreased HDAC4 expression.

HDAC4 Protein Expression in Muscle

The results of immunohistochemical staining showed significant increases in HDAC4 protein expression in both the radiation-induced acute injury ($.67 \pm .22$, $P < .05$) and radiation-induced chronic injury ($.20 \pm .07$, $P < .05$) groups

compared to the control group ($.05 \pm .01$). Compared to the radiation-induced acute injury group, the radiation-induced chronic injury group had significantly lower HDAC4 protein expression ($P < .05$) (Figures 4A–D).

Discussion

Radiation therapy remains an important means of treatment for head and neck cancers such as oral cancer and NPC.^{23,24} However, the complications caused by radiation therapy, including trismus and dysphagia, severely affect patient quality of life.^{25,26} In recent years, radiation-induced muscle injury has become the focus of attention among many researchers. For instance, Hsu et al. investigated the effects of high-dose fractionated irradiation of hind limb muscles of rats administered 6 MV X-rays from a linear accelerator and observed that the irradiated muscles showed progressive structural changes, with muscle cells sustaining injuries from which the rats did not appear to recover.²⁷ Gallet et al. observed fibrosis and inflammatory reactions in the hind limbs of rats administered a single 30-Gy dose of cobalt-60 radiation.²⁸ Zhou et al. established a radiation-induced muscle fibrosis rat model by irradiating the hind limbs of rats with a single 90-Gy dose of radiation and investigated the mechanisms by which radiation caused muscle fibrosis. After irradiation, increased transforming growth factor-beta 1 (TGF- β 1) expression was closely associated with the onset of muscle fibrosis and the proliferation of skeletal muscle satellite cells; moreover, the expression of genes related to myoblast differentiation also gradually increased with time to eventually peak.²⁹ However, the animal experiments described above mainly focused on radiation-induced injury in the skeletal muscles of the hind limb, which is relatively far from the irradiated sites in the clinical treatment of head and neck cancers. Furthermore, most of these studies merely investigated the mechanisms of radiation-induced muscle fibrosis without delving further into the mechanisms of radiation-induced muscle injury. The extent of injury also differed among different radiation equipment. In the present study, we irradiated the TVP muscle region of tree shrews with a 9 MeV electron beam produced by a linear particle accelerator. This was followed by the observation of the pathological changes and measurement of gene and protein expression levels of miR-206 and HDAC4 in the TVP muscle. Previous studies involving the construction of animal models of radiation-induced injury reported animal deaths caused by inappropriate anesthetic doses. Therefore, we administered anesthesia as described in our previous study, which did not lead to any animal deaths due to pre-radiation anesthesia. Thus, a single 20 Gy dose irradiation to the TVP muscle region of tree shrews enabled the successful construction of a tree shrew model of radiation-induced muscle injury. The single-shot anesthesia also reduced the risks associated with anesthesia during the experiment.

In muscle cells that have been irradiated, lipid peroxidation leads to the generation of a series of free radicals, which causes

injury to cell membrane structures and cellular DNA.³⁰ Superoxide dismutases (SODs) are key enzymes that metabolize oxygen radicals to molecular oxygen and malondialdehyde (MDA) is the main metabolite of oxygen radicals. Therefore, SOD and MDA levels can be used to evaluate the degree of radiation-induced cellular injury caused by free radicals.^{31,32} We observed increased MDA expression after radiation-induced injury in the TVP muscle, as well as gradually increased SOD expression during the post-injury repair process. Sun et al. irradiated the unilateral hip of New Zealand white rabbits using 9 MeV electron rays at a single dose of 80 Gy and observed that the area of skeletal muscle fibrosis increased gradually after irradiation.³³ Previous research showed that muscle fibrosis typically starts to occur 2–3 weeks after injury and gradually aggravates over time.³⁴ In the present study, the radiation-induced acute injury group did not show muscle fibrosis, although we did observe decreased capillary count and slight fibrosis in the capillaries. The results in the radiation-induced chronic injury group indicated that the severity of both muscle and capillary fibrosis increased over time, which may be related to the fact that capillaries have poorer tolerance to radiation compared to skeletal muscle. Functional decline gradually occurs in muscles with the accumulation of radiation dose over time. This may be related to factors such as the slow and incomplete repair of capillaries that are injured when capillary networks in the gaps between muscle fibers are subjected to irradiation.^{35,36} Clinical research has demonstrated that a reduction in the number of capillaries and capillary fibrosis also results in tissue injury,³⁷ suggesting that the decreased capillary count and occurrence of fibrosis may be related to the progression of radiation-induced muscle injury, the reduced number of capillaries and capillary fibrosis may have aggravated the muscle tissue injury in the radiation-induced tree shrew model of muscle injury.

MiR-206 is mainly expressed in newly formed myotubes and regenerated muscle fibers.³⁸ Liu et al.³⁹ demonstrated that miR-206 regulates satellite cell differentiation and that its deficiency may cause a delay in skeletal muscle regeneration and maturation in mice. HDAC4 is a target gene of miRNAs that participate in myogenesis. Being highly expressed in muscle tissues, HDAC4 participates in the inhibition of myogenic differentiation in myoblasts through the mediation of miR206 function.^{40,41} Therefore, we surmised that the miR-206 pathway may also play a role in the progression of radiation-induced muscle injury. In the present study, the radiation-induced acute injury group showed downregulation of miR-206 expression and upregulation of HDAC4 expression, indicating the occurrence of radiation-induced injury in muscle tissue. With miR-206 upregulation, HDAC4 expression decreased, indicating the occurrence of gradual muscle repair after injury. Therefore, the mechanisms of radiation-induced muscle injury may be the inhibition of muscle repair and regeneration by miR-206 through the regulation of HDAC4, which leads to muscle atrophy and

fibrosis. Previous studies have also reported that miR-206 expression is regulated by TGF- β ,^{42,43} which is closely associated with radiation-induced muscle fibrosis. However, further research is required to determine whether TGF- β participates in radiation-induced muscle injury and whether it regulates miR-206 in radiation-induced muscle injury.

The irradiated tree shrews in the present study also exhibited obvious injury to the pseudostratified ciliated columnar epithelium; relatively disorderly arrangements of epithelial cells; lodging and partial detachment of cilia in the auditory vesicles; and epithelial detachment, serous fluid, disorderly epithelial cell arrangements, and cilia detachment in the lumen of the Eustachian tube. The micro-CT revealed radiation-induced secretory otitis media in several tree shrews ($n = 3$). Contrary to the processes reported by Ohashi et al.^{44,45} who constructed rat models of radiation-induced secretory otitis media, the onset of secretory otitis media in the present study was caused by the irradiation of the TVP muscle region of tree shrews. Previous research has shown that the occurrence of radiation-induced secretory otitis media is related to Eustachian tube dysfunction (i.e., abnormal opening of the Eustachian tube). Since the TVP muscle is the main muscle responsible for controlling the opening of the Eustachian tube, radiation-induced TVP muscle injury is one likely cause of radiation-induced secretory otitis media.⁴⁶ Therefore, the present study provides a novel approach to the construction of animal models of radiation-induced secretory otitis media. The following experiments will investigate the relationship between post-radiation secretory otitis media and muscle damage, providing new possibilities for reducing the occurrence of post-radiation secretory otitis media. In this study, we verified the changes of the miR-206 pathway in radiation-induced muscle injury. We hope to regulate the miR-206 pathway in cells further and observe the effect of up-regulation or down-regulation miR-206 on cells after radiation. We tried different methods to isolate and purify tree shrew myoblasts during the experiment. However, we could not overcome the difficulties, such as the rapid growth of fibroblasts and contamination of cells. In the subsequent experiments, we will try more ways to culture myoblasts.

Conclusion

In this study, a tree shrew model of radiation induced-muscle injury was established by 20 Gy dosage. Studies have found that radiation can lead to oxidative damage, decreased capillaries, and muscle fibrosis. Although partial repair of the TVP muscle occurs over time, it is insufficient to offset the damage caused by radiation. By regulating the expression of HDAC4, the miR-206 pathway is considered an essential player in muscle radiation injury. The pathway will provide a new target for the prevention of radiation muscle damage.

Acknowledgments

We thank the Kunming zoology institute, Chinese Academy of Science for providing experiment animal sources and the Experimental Animal Center of Guangxi Medical University for providing technical support for animal feeding. We thank the members of our research groups for providing technical Assistance and participating in discussions

Author's Note

Pengcheng Zhao and Wei Xia contributed equally to this work and should be considered co-first authors.

Declaration of Conflicting Interests

The author(s) declared no potential conflicts of interest with respect to the research, authorship, and/or publication of this article.

Funding

The author(s) disclosed receipt of the following financial support for the research, authorship, and/or publication of this article: This work was supported by the National Natural Science Foundation of China (Grant No. 81760189); the Innovation Project of Guangxi Graduate Education (Grant No. YCSW2021127); College Student's Innovation and Entrepreneurship Training Program (Grant No. 202010598053); Guangxi Clinic Medicine Research Center of Nasopharyngeal Carcinoma (Grant No. GuikeAD20297078); Guangxi Natural Science Foundation Program (Grant No. 2020GXNSFAA297235); Guangxi Scholarship Fund of Guangxi Education Department of China.

ORCID iD

Pengcheng Zhao  <https://orcid.org/0000-0002-0189-0119>

References

1. Shield KD, Ferlay J, Jemal A, et al. The global incidence of lip, oral cavity, and pharyngeal cancers by subsite in 2012. *CA Cancer J Clin*. 2017 Jan;67(1):51-64. doi:10.3322/caac.21384.
2. Hu CY, Wang WM, Chu XH, Ren ZH, Lyu J. Global, regional, and national burden of nasopharyngeal carcinoma from 1990 to 2017-results from the global burden of disease study 2017. *Head Neck*. 2020 Nov;42(11):3243-3252. doi:10.1002/hed.26378.
3. Refaat T, Choi M, Thomas TO, et al. Whole-field sequential intensity-modulated radiotherapy for local-regional advanced head-and-neck squamous cell carcinoma. *Am J Clin Oncol*. 2015 Dec;38(6):588-594. doi:10.1097/COC.000000000000001.
4. Yi JL, Gao L, Huang XD, et al. Nasopharyngeal carcinoma treated by radical radiotherapy alone: Ten-year experience of a single institution. *Int J Radiat Oncol Biol Phys*. 2006 May 1; 65(1):161-168. doi:10.1016/j.ijrobp.2005.12.003.
5. Cheung JPY, Wei WI, Luk KDK. Cervical spine complications after treatment of nasopharyngeal carcinoma. *Eur Spine J*. 2012; 22(3):584-592. doi:10.1007/s00586-012-2600-9.
6. Straub JM, New J, Hamilton CD, Lominska C, Shnayder Y, Thomas SM. Radiation-induced fibrosis: mechanisms and

- implications for therapy. *J Cancer Res Clin Oncol*. 2015 Nov; 141(11):1985-1994. doi:10.1007/s00432-015-1974-6.
7. Liao W, Zheng Y, Bi S, et al. Carotid stenosis prevalence after radiotherapy in nasopharyngeal carcinoma: A meta-analysis. *Radiother Oncol*. 2019 Apr;133:167-175. doi:10.1016/j.radonc.2018.11.013.
 8. Russell JA, Connor NP. Effects of age and radiation treatment on function of extrinsic tongue muscles. *Radiat Oncol*. 2014 Dec 4; 9:254. doi:10.1186/s13014-014-0254-y.
 9. Ghosh PS, Milone M. Clinical and laboratory findings of 21 patients with radiation-induced myopathy. *J Neurol Neurosurg Psychiatry*. 2015 Feb;86(2):152-158. doi:10.1136/jnnp-2013-307447.
 10. Meheissen MAM, Mohamed ASR, Kamal M, et al. A prospective longitudinal assessment of MRI signal intensity kinetics of non-target muscles in patients with advanced stage oropharyngeal cancer in relationship to radiotherapy dose and post-treatment radiation-associated dysphagia: Preliminary findings from a randomized trial. *Radiother Oncol*. 2019 Jan; 130:46-55. doi:10.1016/j.radonc.2018.08.010.
 11. Seidel C, Kuhnt T, Kortmann RD, Hering K. Radiation-induced campyocormia and dropped head syndrome: Review and case report of radiation-induced movement disorders. *Strahlenther Onkol*. 2015 Oct;191(10):765-770. doi:10.1007/s00066-015-0857-8.
 12. Baoge L, Van Den Steen E, Rimbaut S, et al. Treatment of skeletal muscle injury: A review. *ISRN orthopedics*. 2012;2012: 1-7. doi:10.5402/2012/689012.
 13. Chen JF, Tao Y, Li J, et al. microRNA-1 and microRNA-206 regulate skeletal muscle satellite cell proliferation and differentiation by repressing Pax7. *J Cell Biol*. 2010 Sep 6;190(5): 867-879. doi:10.1083/jcb.200911036.
 14. Kim HK, Lee YS, Sivaprasad U, Malhotra A, Dutta A. Muscle-specific microRNA miR-206 promotes muscle differentiation. *J Cell Biol*. 2006 Aug 28;174(5):677-687. doi:10.1083/jcb.200603008.
 15. Nakasa T, Ishikawa M, Shi M, Shibuya H, Adachi N, Ochi M. Acceleration of muscle regeneration by local injection of muscle-specific microRNAs in rat skeletal muscle injury model. *J Cell Mol Med*. 2010 Oct;14(10):2495-2505. doi:10.1111/j.1582-4934.2009.00898.x.
 16. Williams AH, Valdez G, Moresi V, et al. MicroRNA-206 delays ALS progression and promotes regeneration of neuromuscular synapses in mice. *Science*. 2009 Dec 11;326(5959):1549-1554. doi:10.1126/science.1181046.
 17. Fan Y, Huang ZY, Cao CC, et al. Genome of the Chinese tree shrew. *Nat Commun*. 2013;4(1). doi:10.1038/ncomms2416.
 18. Cao J, Yang EB, Su JJ, Li Y, Chow P. The tree shrews: Adjuncts and alternatives to primates as models for biomedical research. *J Med Primatol*. 2003 Jun;32(3):123-130. doi:10.1034/j.1600-0684.2003.00022.x.
 19. Zheng Y, Yun C, Wang Q, Smith WW, Leng J. Identification of the full-length β -actin sequence and expression profiles in the tree shrew (*Tupaia belangeri*). *Int J Mol Med*. 2015 Feb;35(2): 519-524. doi:10.3892/ijmm.2014.2040.
 20. Gao Y, Tang A, Liu J, Wang X, He G, Min Z. [Analysis on the relationship between tensor veli palatini and secretory otitis media in patients with nasopharyngeal carcinoma after radiotherapy]. *Lin chuang er bi yan hou tou jing wai ke za zhi*. 2010 Aug;24(16):743-745.
 21. Gyanwali B, Li H, Xie L, et al. The role of tensor veli platini muscle (TVP) and levator veli platini muscle (LVP) in the opening and closing of pharyngeal orifice of Eustachian tube. *Acta Oto-Laryngologica*. 2016;136(3):249-255. doi:10.3109/00016489.2015.1107192.
 22. Xia W, Huang ZJ, Feng YW, Tang AZ, Liu L. Body surface area-based equivalent dose calculation in tree shrew. *Sci Prog*. 2021 Apr-Jun;104(2):003685042110169. doi:10.1177/00368504211016935.
 23. Liao CT, Chang JT, Wang HM, et al. Does adjuvant radiation therapy improve outcomes in pT1-3N0 oral cavity cancer with tumor-free margins and perineural invasion? *Int J Radiat Oncol Biol Phys*. 2008 Jun 1;71(2):371-376. doi:10.1016/j.ijrobp.2007.10.015.
 24. Wei WI, Sham JS. Nasopharyngeal carcinoma. *Lancet (London, England)*. 2005 Jun 11-17;365(9476):2041-2054. doi:10.1016/s0140-6736(05)66698-6.
 25. Lalla RV, Treister N, Sollecito T, et al. Oral complications at 6 months after radiation therapy for head and neck cancer. *Oral Dis*. 2017 Nov;23(8):1134-1143. doi:10.1111/odi.12710.
 26. Tolentino Ede S, Centurion BS, Ferreira LH, Souza AP, Damante JH, Rubira-Bullen IR. Oral adverse effects of head and neck radiotherapy: Literature review and suggestion of a clinical oral care guideline for irradiated patients. *J Appl Oral Sci*. 2011 Oct;19(5):448-454. doi:10.1590/s1678-77572011000500003.
 27. Hsu HY, Chai CY, Lee MS. Radiation-induced muscle damage in rats after fractionated high-dose irradiation. *Radiat Res*. 1998 May;149(5):482-486.
 28. Gallet P, Phulpin B, Merlin JL, et al. Long-term alterations of cytokines and growth factors expression in irradiated tissues and relation with histological severity scoring. *PLoS One*. 2011; 6(12):e29399. doi:10.1371/journal.pone.0029399.
 29. Zhou Y, Sheng X, Deng F, et al. Radiation-induced muscle fibrosis rat model: Establishment and valuation. *Radiat Oncol*. 2018 Aug 29;13(1):160. doi:10.1186/s13014-018-1104-0.
 30. Aryafar T, Amini P, Rezapoor S, et al. Modulation of Radiation-Induced NADPH Oxidases in Rat's Heart Tissues by Melatonin. *Journal of Biomedical Physics and Engineering*. 2021 Aug; 11(4):465-472. doi:10.31661/jbpe.v0i0.1094.
 31. Zheng X, Li L, Zhu Y, et al. Superoxide dismutase predicts persistent circulation failure and mortality in the early stage of acute pancreatitis. *Dig Dis Sci*. 2020 Dec;65(12):3551-3557. doi:10.1007/s10620-020-06069-w.
 32. Djordjevic A, Kotnik P, Horvat D, Knez Z, Antonic M. Pharmacodynamics of malondialdehyde as indirect oxidative stress marker after arrested-heart cardiopulmonary bypass surgery. *Biomed Pharmacother*. 2020 Dec;132:110877. doi:10.1016/j.biopha.2020.110877.
 33. Sun W, Ni X, Sun S, et al. Adipose-derived stem cells alleviate radiation-induced muscular fibrosis by suppressing the expression of TGF- β 1. *Stem Cells International*. 2016;2016:1-9. doi:10.1155/2016/5638204.

34. Huard J, Li Y, Fu FH. Muscle injuries and repair: Current trends in research. *J Bone Jt Surg Am Vol.* 2002 May;84(5): 822-832.
35. Nichol AM, Smith SL, D'Yachkova Y, et al. Quantification of masticatory muscle atrophy after high-dose radiotherapy. *Int J Radiat Oncol Biol Phys.* 2003 Jul 15;56(4):1170-1179. doi:10.1016/s0360-3016(03)00118-4.
36. Dewhirst MW. Relationships between cycling hypoxia, HIF-1, angiogenesis and oxidative stress. *Radiat Res.* 2009 Dec;172(6): 653-665. doi:10.1667/rr1926.1.
37. Dorresteijn LD, Kappelle AC, Boogerd W, et al. Increased risk of ischemic stroke after radiotherapy on the neck in patients younger than 60 years. *J Clin Oncol.* 2002 Jan 1;20(1):282-288. doi:10.1200/jco.2002.20.1.282.
38. Yuasa K, Hagiwara Y, Ando M, Nakamura A, Takeda S, Hijikata T. MicroRNA-206 is highly expressed in newly formed muscle fibers: implications regarding potential for muscle regeneration and maturation in muscular dystrophy. *Cell Structure and Function.* 2008;33(2):163-169. doi:10.1247/csf.08022.
39. Liu N, Williams AH, Maxeiner JM, et al. microRNA-206 promotes skeletal muscle regeneration and delays progression of Duchenne muscular dystrophy in mice. *J Clin Invest.* 2012 Jun;122(6):2054-2065. doi:10.1172/JCI62656.
40. McKinsey TA, Zhang CL, Lu J, Olson EN. Signal-dependent nuclear export of a histone deacetylase regulates muscle differentiation. *Nature.* 2000 Nov 2;408(6808):106-111. doi:10.1038/35040593.
41. Kirby TJ, McCarthy JJ. MicroRNAs in skeletal muscle biology and exercise adaptation. *Free Radic Biol Med.* 2013 Sep;64: 95-105. doi:10.1016/j.freeradbiomed.2013.07.004.
42. Winbanks CE, Wang B, Beyer C, et al. TGF- β regulates miR-206 and miR-29 to control myogenic differentiation through regulation of HDAC4. *J Biol Chem.* 2011 Apr 22;286(16): 13805-13814. doi:10.1074/jbc.M110.192625.
43. Pan Y, Liu L, Li S, et al. Activation of AMPK inhibits TGF- β 1-induced airway smooth muscle cells proliferation and its potential mechanisms. *Sci Rep.* 2018 Feb 26;8(1):3624. doi:10.1038/s41598-018-21812-0.
44. Ohashi Y, Nakai Y, Esaki Y, Ikeoka H, Koshimo H, Onoyama Y. Acute effects of irradiation on middle ear mucosa. *The Annals of otology, rhinology, and laryngology.* 1988 Mar-Apr;97(2 Pt 1): 173-178. doi:10.1177/000348948809700215.
45. Ohashi Y, Nakai Y, Ikeoka H, Esaki Y, Koshimo H, Onoyama Y. Mucosal pathology of an experimental otitis media with effusion after X-ray irradiation. *Am J Otolaryngol.* 1987 Jul-Aug;8(4): 223-235. doi:10.1016/s0196-0709(87)80008-x.
46. Zhou Y, Tang A, Li J, Chen P, Mao R. [The damaged types of eustachian tube function in the patients of nasopharyngeal carcinoma after radiotherapy]. *Lin chuang er bi yan hou ke za zhi.* 2003 Aug;17(8):464-465.